High-temperature phase in zirconia film fabricated by aerosol gas deposition and its change upon subsequent heat treatment

Eiji FUCHITA,[*,**,****,†] Eiji TOKIZAKI,[**,****] Eiichi OZAWA,[**,****]
Hirofumi INOUE,[***] Yoshio SAKKA[*,****] and Eiji KITA[*]

*School of Pure and Applied Science, University of Tsukuba, 1–1–1 Tennodai, Tsukuba, Ibaraki 305–8573, Japan
**Fuchita Nanotechnology, Ltd., 2–25–57 Tamatsukuri, Narita, Chiba 286–0011, Japan
***Osaka Prefecture University, 1–1 Gakuen-cho, Naka-ku, Sakai 599–8531, Japan
****National Institute for Materials Science, 1–2–1 Sengen, Tsukuba, Ibaraki 305–0047, Japan

A zirconia film synthesized by aerosol gas deposition (AGD) contains a high-temperature phase of zirconia even if synthesized at room temperature. We attempted to clarify the change of the high-temperature phase upon subsequent heat treatment using zirconia powder with a mean particle diameter of 7.7 μm obtained by the dry method. X-ray diffraction (XRD) analysis was used to examine the crystal structure evolution of the AGD zirconia film during heat treatment, and a high-temperature XRD system was also used to measure crystal size at various heating temperatures. The as-deposited zirconia AGD film was found to be composed of monoclinic crystallites about 10 nm in diameter and tetragonal crystallites about 6 nm in diameter. The tetragonal crystallites were stable up to 1373 K, increasing their diameters to 14 nm upon heating. Then, the internal stress of the AGD zirconia film as well as the effects of heating temperature and holding time on internal stress were evaluated. The internal stress induced in the zirconia AGD film was 1.7 GPa, which decreased only up to 1.4 GPa after heat treatment at 1473 K.

1. Introduction

Ceramics fabrication by aerosol gas deposition (AGD) is completely different from conventional ceramic fabrication, in which samples are treated at more than 1273 K to form ceramic compacts or ceramic films. In AGD, ceramic powder is synthesized into bulk ceramics simply by injecting it from a nozzle onto a substrate.[1)–5)] During the fabrication of AGD films, we have observed luminescence, which we concluded to be due to static electricity induced by the friction between powder particles, the carrier tubing and the nozzle.[6)] The advantage of AGD over other methods such as sputtering, plasma chemical vapor deposition and laser chemical vapor deposition is its low temperature.[7)] Hence, AGD is expected to be applied to the formation of ceramic coatings on metal surfaces and to the manufacture of insulating films and electrical devices such as fuel cells.

Zirconia has a monoclinic phase at room temperature, which undergoes a transition to tetragonal phase above 1273 K. The phase transition is associated with a 4% reduction in volume, indicating that repeated cycles of heating and cooling will lead to the fracture of zirconia crystals, as shown in **Table 1**. This phenomenon is prevented by stabilizing the tetragonal phase at room temperature by adding oxides such as calcium oxide,[8)] magnesium oxide[8)] and yttrium oxide.[8),9)] Therefore, for pure zirconia, its crystal structure is generally monoclinic at room temperature.

We found that the tetragonal structure is formed in zirconia films synthesized by AGD[6),10)–12)] and that the generation of the high-temperature phase does not depend on the method (i.e., wet or dry method) used to manufacture zirconia powder.[10),11)] However, the high-temperature phase is more prevalent in zirconia powder produced by the dry method with a mean particle diameter of 7.7 μm.[6)] In AGD, because samples are prepared at room temperature, the appearance of the high-temperature phase is unexpected. In previous research on zirconia growth, the appearance of the high-temperature phase has been examined by considering the effects of particle size,[13)–17)] oxygen deficit[18)–20)] and pressure during fabrication.[21),22)]
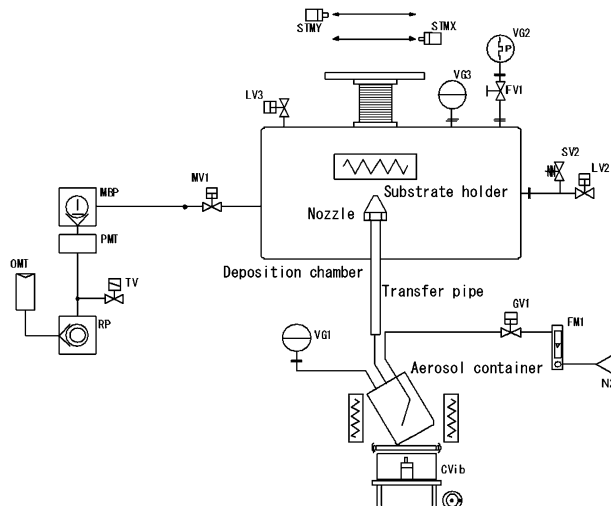
In this study, we attempted to clarify the phase transition behavior upon subsequent heat treatment of the high-temperature phase at room temperature using zirconia powder with a particle diameter of 7.7 μm formed by the dry method.

2. Experimental procedure

2.1 Materials used

The zirconia powder used was produced by Daiichi Kigenso Kagaku Co. Ltd., by the dry method. According to its specifications, the powder has a mean particle diameter of 7.7 μm and

Table 1. Lattice parameters for zirconia

	Monoclinic		Face-centered tetragonal (fct)	
	At room temperature[25)]	At 1229 K[26)]		At 1425 K[26)]
a	0.51507 nm	0.51882 nm	a	0.51518 nm
b	0.52031 nm	0.52142 nm		
c	0.53154 nm	0.53836 nm	c	0.52724 nm
β	99.194°	98.783°		
	Unit cell volumes			
	0.14062 nm³	0.14393 nm³		0.13993 nm³

† Corresponding author: E. Fuchita; E-mail: fuchita@nanotechjp.com

Fig. 1.   Schematic diagram of AGD apparatus.[10]

Fig. 2.   XRD profiles of annealed AGD zirconia films and original powder.

a specific surface area of $1.6\,m^2/g$.[11] The powder obtained was dried in a heat treatment furnace to standardize its humidity level before starting AGD.

2.2   Experimental apparatus

Figure 1 shows a schematic diagram of the AGD apparatus. Zirconia powder was set in an aerosol container made of glass and equipped with a gas-supplying apparatus. When gas is supplied near the bottom of the container, the powder is blown into a film formation chamber through a tubing. The powder is ejected onto a $25 \times 25\,mm^2$ alumina substrate through a nozzle of 30 mm width. The substrate is controlled by a drive unit so that it undergoes reciprocating motion at a speed of 1 mm/s.

2.3   Conditions for film synthesis and evaluation method

Zirconia films were synthesized on alumina substrates and then annealed at a temperature raised from 873 to 1473 K at a rate of 0.16 K/s. The sample films were maintained at the given temperature for 1.8 ks (0.5 h) to 10.8 ks (3 h). Scanning electron microscopy (SEM, JEOL) and X-ray diffractometry (XRD, Rigaku) were used to analyze the crystal structure of the samples. A surface texture and contour measuring instrument (Tokyo Seimitsu; SURFCOM 480B) and a micrometer (Mitutoyo) were also used to measure film surface morphology and film thickness, respectively. For all the films, internal stress was obtained from the curvature of the films using Stoney's formula,[23),24)] and crystal size was calculated using Scherrer's equation. In this paper, monoclinic crystallites of 10.3 nm size and tetragonal crystallites of 6.0 nm size are denoted m-10.3 and t-6.0 nm, respectively. Moreover, the annealing temperature at 1473 K and the XRD measuring temperature at 1273 K are denoted Ta = 1473 K and Tm = 1273 K, respectively.

3.   Results

3.1   XRD results

3.1.1   XRD profiles of annealed zirconia films and heating process

Five zirconia films were used to examine the effect of heat treatment on crystal structure. Here, the sample films were subjected to annealing at Ta = 1073, 1173, 1273, 1373 and 1473 K for 1.8 ks. The XRD profiles of the as-deposited sample and five
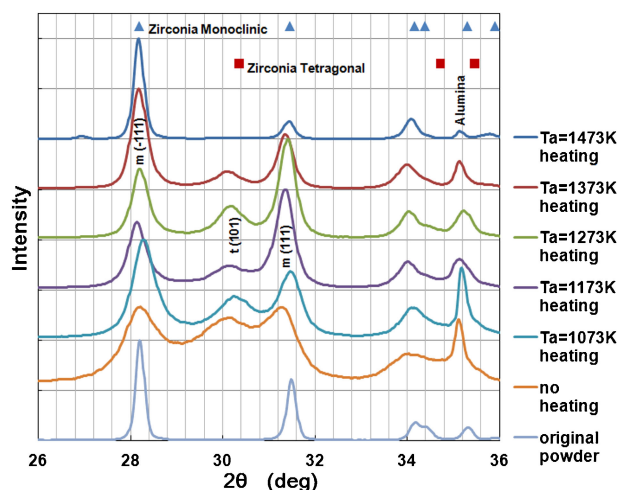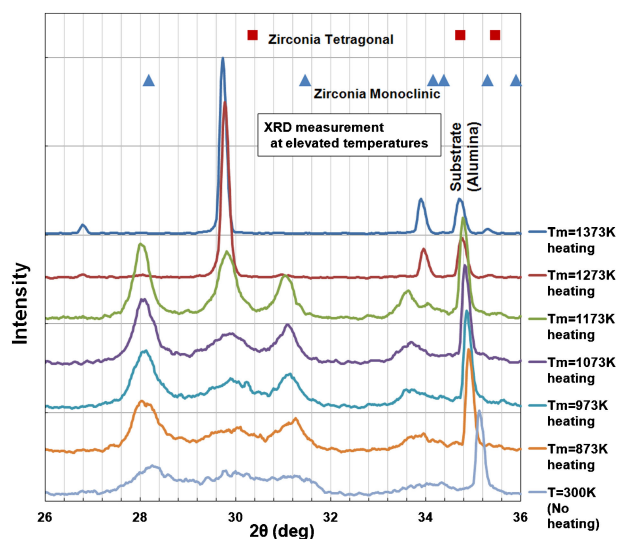

Fig. 3.   XRD profiles of AGD zirconia films at elevated temperatures.

samples after cooling from their respective heating temperatures to room temperature as well as the XRD profile of the original powder (100% monoclinic) are shown in **Fig. 2**. The XRD peaks of the monoclinic phase become sharp with an increment in heating temperature. However, the peak of the tetragonal phase remains broad. The tetragonal phase remains even in the sample annealed at Ta = 1373 K. In the sample annealed at Ta = 1473 K, the tetragonal phase disappears and only the monoclinic phase remains.

The structural changes of the AGD sample films were examined at a temperature raised from Tm = 873 K to Tm = 1373 K at 100 K intervals using a high-temperature XRD system. The XRD profile obtained at each temperature was compared with the XRD profile obtained at room temperature. The heating rate was 0.167 K/s and the holding time was 1.8 ks for each heating temperature. The experimentally obtained high-temperature XRD profiles are shown in **Fig. 3**. The XRD peaks of the monoclinic phase almost disappeared at Tm = 1273 K and the tetragonal peaks increased in area above Tm = 1173 K.

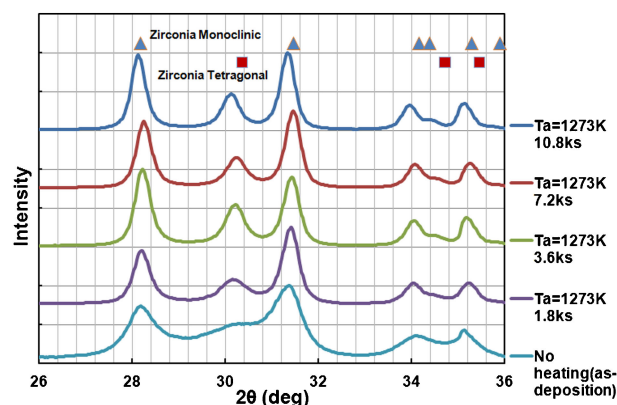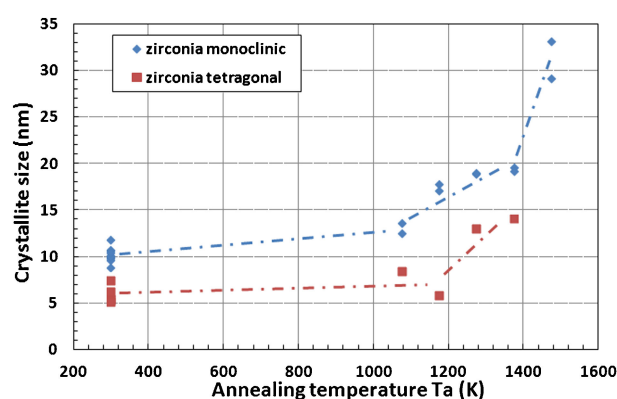Fig. 4. Effect of holding time on structure of crystallites in AGD zirconia film.

Fig. 6. Crystallite sizes at elevated temperatures.

Fig. 5. Relation between crystallite size and annealing temperature.

Fig. 7. Relationship between crystallite size and holding time.

The XRD profiles obtained for holding times of 1.8, 3.6, 7.2 and 10.8 ks at Ta = 1273 K are shown in **Fig. 4**. After holding for 10.8 ks at Ta = 1273 K, the tetragonal structure remained.

3.1.2 Crystallite size of annealed films and at elevated temperatures

Crystallite diameter was calculated by applying Scherrer's equation to the XRD data using Rigaku's PDXL software. The estimated sizes of the (−111) (111) monoclinic and (101) tetragonal crystallites are shown in **Fig. 5**. The crystallite sizes of the as-deposited AGD zirconia film were m-10 nm (max: 12 nm, min: 9 nm) for the monoclinic phase and t-6 nm (max: 8 nm, min: 5 nm) for the tetragonal phase. These crystallite sizes are nearly equal to the particle sizes of 5 to 10 nm in the transmission electron microscopy images.[12] The crystallite sizes for the monoclinic and tetragonal phases do not change up to Ta = 1073 K. Both sizes increased with increasing temperature from Ta = 1173 K. When annealing temperature was increased from Ta = 1373 K to Ta = 1473 K, monoclinic crystallite size increased from m-20 to m-31 nm. Tetragonal crystallite size increased to up to t-14 nm at Ta = 1373 K.

The crystallite sizes estimated from the (−111) (111) monoclinic and (101) tetragonal structures are shown in **Fig. 6**. The sizes of zirconia crystallites obtained by AGD were m-9 nm for the monoclinic structure and t-12 nm for the tetragonal structure at 300 K. At Tm = 1173 K, the monoclinic crystallite size was m-22 nm and the tetragonal crystallite size was t-20 nm. A rapid growth of the tetragonal crystallites occurred at Tm = 1273 K and above, resulting in the formation of only tetragonal crys-
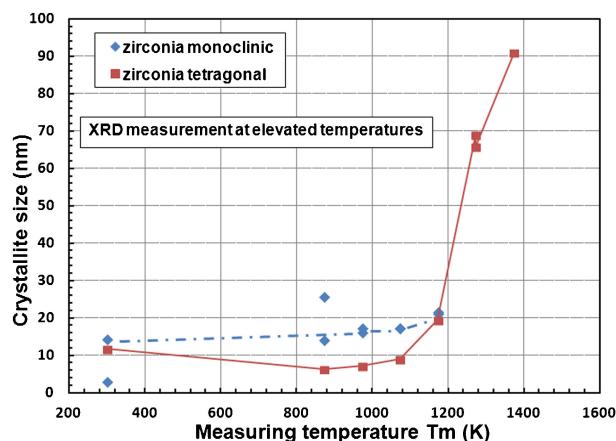
tallites. The tetragonal crystallite sizes at Tm = 1273 K and Tm = 1373 K were t-67 and t-91 nm, respectively.

For holding times of 1.8, 3.6, 7.2 and 10.8 ks at Ta = 1273 K, the crystallite sizes estimated from the (−111) (111) monoclinic and (101) tetragonal structures are shown in **Fig. 7**. Both monoclinic and tetragonal crystallite sizes nearly saturated within 1 h. After 3 h of holding, the monoclinic and tetragonal crystallite sizes were m-23 and t-19 nm, respectively.

3.2 Internal stress induced in zirconia film obtained by AGD and effect of annealing

The internal stresses of the as-deposited and annealed films are shown in **Fig. 8**. The average internal stress of the as-deposited zirconia film was 1.7 GPa which decreased to 0.8 GPa with annealing at approximately Ta = 1173 K. However, it increased to 1.4 GPa after annealing at Ta = 1473 K with a 1.8 ks holding time.

The change in internal stress with holding time at Ta = 1273 K is shown in **Fig. 9**. Internal stress decreased up to a holding time of 7.2 ks. However, it increased when holding time was further increased to 10.8 ks.

3.3 SEM observation of microstructure of zirconia films

SEM images of the fracture surface of the zirconia films after annealing are shown in **Fig. 10**. The SEM image of the film subjected to annealing at Ta = 1073 K indicated the existence of fine particles less than 100 nm in diameter. At Ta = 1273 K, the
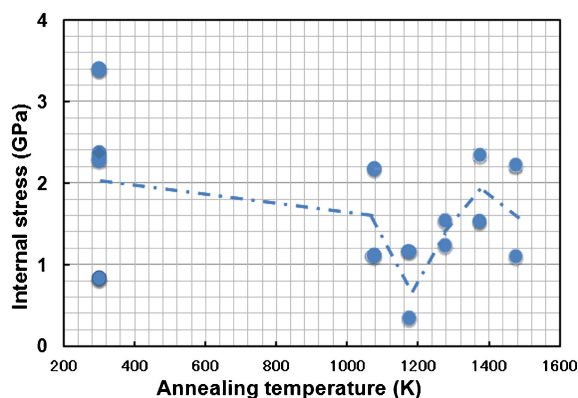
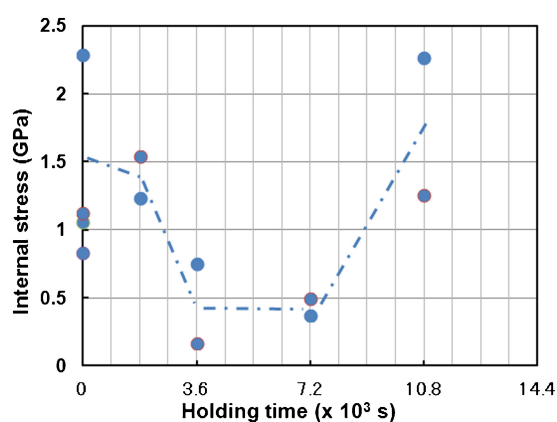Fig. 8. Internal stress in AGD zirconia film as function of annealing temperature.

Fig. 9. Internal stress in AGD zirconia film as function of holding time at Ta = 1273 K.

Fig. 10. SEM images of AGD zirconia films heated at (A) Ta = 1073 K, (B) Ta = 1173 K, (C) Ta = 1273 K and (D) Ta = 1473 K (holding time: 1.8 ks).

Fig. 11. SEM images of AGD zirconia films heated at Ta = 1273 K for (A) 7.2 ks and (B) 10.8 ks.

film appeared to be dense although cracks were formed. Finally, at Ta = 1473 K, a rapid particle growth occurred, resulting in the formation of particles 600 to 700 nm in diameter.

SEM images of the fracture surface of the films heated at Ta = 1273 K with different holding times are shown in **Fig. 11**. Heat treatment for 7.2 ks appeared to introduce pores into the films because hollow regions could be observed. However, the density appeared to be higher in the film heated for 10.8 ks.

4. Discussion

The as-deposited AGD film contains monoclinic and tetragonal crystallites. The sizes of the monoclinic and tetragonal crystallites are m-10 and t-6 nm, respectively. The tetragonal crystallites were of high-temperature phase. Generally, they exist at more than Ta = 1473 K. However, in this study, their sizes were estimated to be approximately 6 nm. According to previous researchers,[13]–[17] zirconia crystallites less than 30 nm in size are stable at room temperature. Thus, the appearance of the high-temperature phase (tetragonal phase) in the as-deposited AGD film could only be explained by the crystallite size of t-6 nm. Crystallite size is constant during heating up to Ta = 1073 K, as shown in Fig. 5. That is, the as-deposited state is maintained up to Ta = 1073 K. Crystallite size clearly increases with heating above Ta = 1173 K, as shown in Fig. 5. The densification of AGD films starts above Ta-1173 K. We can see the densification aspect of the film in the SEM images in Fig. 10.

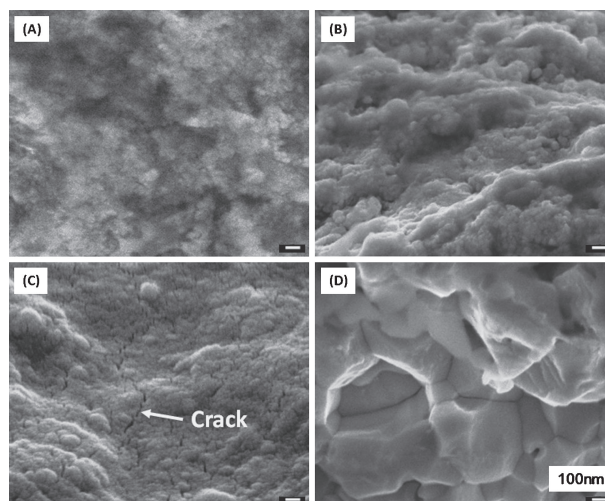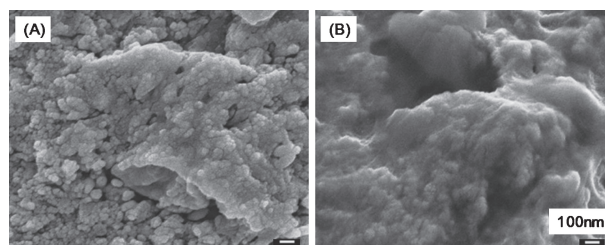The tetragonal phase disappeared in the film cooled from Ta = 1473 K in Fig. 2. However, both the monoclinic and tetragonal phases exist in the film cooled from less than Ta = 1373 K. On the other hand, in the in situ XRD profile shown in Fig. 3, the monoclinic phase has already disappeared between Tm = 1273 K and Tm = 1373 K, although the monoclinic phase appeared in the film cooled from this temperature range. This experimental result indicates that the tetragonal phase separates into the monoclinic and tetragonal phases during cooling. The AGD films heated between Tm = 1273 K and Tm = 1373 K were composed of tetragonal crystallites more than t-70 nm in diameter, formed by the phase transformation of monoclinic crystallites, and relatively small tetragonal crystallites less than t-14 nm in diameter, as determined from the SEM images and XRD analysis data of crystallite size. It is concluded that the crystallites more than t-70 nm in diameter transform to monoclinic crystallites and that crystallites less than t-14 nm in diameter remain during cooling to room temperature.

Concerning the internal stress induced in the AGD films, it decreases at approximately Ta = 1173 K, as shown in Fig. 9 and Fig. 11. This internal stress decrease might be induced by the densification of the as-deposited film. However, the film heat-treated at much higher temperatures exhibited a high thermal residual stress, i.e., 1.4 GPa, which is considered to depend on the phase transformation from the tetragonal phase to the monoclinic phase.

5. Conclusions

1. As-deposited zirconia AGD films are composed of monoclinic crystallites about m-10 nm in diameter and tetragonal

crystallites about t-6 nm in diameter. The films are stable up to approximately Ta = 1073 K, and the grain growth of their crystallites starts above Ta = 1173 K.

2. According to in situ XRD analysis results, all monoclinic crystallites transform to tetragonal ones. However, AGD films contain monoclinic and tetragonal crystallites during cooling to room temperature. AGD films heated above Ta = 1473 K contain only monoclinic crystallites. Whether heat-treated AGD films exhibit a monophase or a mixture of phases depends on the crystallite size distribution in the film. If crystallites several nanometers in size exist, AGD films will have a two-phase structure.

3. The internal stress of 1.7 GPa induced in as-deposited AGD films decreases to 0.8 GPa with annealing at approximately Ta = 1173 K. However, such stress cannot be removed by the heat treatment of the films because thermal residual stress (1.4 GPa) is induced in the films even during cooling. The thermal stress will depend on the transformation from the tetragonal phase to the monoclinic phase.

References

1) S. Kashu, E. Fuchita, T. Manabe and C. Hayashi, *Jpn. J. Appl. Phys.*, **23**, L910–L912 (1984).

2) S. Kashu, Y. Matsuzaki, M. Kaito, M. Toyokawa, K. Hatanaka and C. Hayashi, "Preparation of Superconducting Thick Films of Bi-Pb-Sr-Ca-Cu-O by Gas Deposition of Fine Powder", Proceedings of the 2nd International Symposium on Superconductivity (ISS89), Tsukuba, Japan (1989) pp. 413–418.

3) C. Hayashi, *Mater. Sci. Forum*, **246**, 153–180 (1997).

4) S. Kashu and Y. Mihara, *J. Jpn. Soc. Powder Metallurgy*, **42**, 314–317 (1995).

5) J. Akedo, *J. Therm. Spray Technol.*, **17**, 181–198 (2008).

6) E. Fuchita, E. Tokizaki, E. Ozawa and Y. Sakka, *J. Ceram. Soc. Japan*, **119**, 271–276 (2011).

7) T. Goto, *J. Surf. Finish. Soc. Jpn.*, **60**, 709–715 (2009).

8) S. Somiya, N. Yamamoto and H. Yanagida: Science and Technology of Zirconia 3 (Advances in Ceramics, 24A), American Ceramic Society (1988).

9) O. Vasylkiv, Y. Sakka, Y. Maeda and V. V. Skorokhod, *J. Am. Ceram. Soc.*, **88**, 639–644 (2005).

10) E. Fuchita, E. Tokizaki and Y. Sakka, *J. Ceram. Soc. Japan*, **118**, 767–770 (2010).

11) E. Fuchita, E. Tokizaki, E. Ozawa and Y. Sakka, *J. Ceram. Soc. Japan*, **118**, 948–951 (2010).

12) E. Fuchita, E. Tokizaki, E. Ozawa and Y. Sakka, *J. Jpn. Soc. Powder Metallurgy*, **58**, 463–472 (2011) [in Japanese].

13) R. C. Garvie, *J. Phys. Chem.*, **69**, 1238–1243 (1965).

14) I-Wei Chen, Y-H. Chiao and K. Tsuzaki, *Acta Metall.*, **33**, 1847–1859 (1985).

15) E. Djurado, P. Bouvier and G. Lucazeau, *J. Solid State Chem.*, **149**, 399–407 (2000).

16) M. W. Pitcher, S. V. Ushakov, A. Navrotsky, B. F. Woodfield, G. S. Li, J. Boerio-Goates and B. M. Tissue, *J. Am. Ceram. Soc.*, **88**, 160–167 (2005).

17) D. G. Lamas, A. M. Rosso, M. S. Anzorena, A. Fernandez, M. G. Bellino, M. D. Cabezas, N. E. Walsoe de Reca and A. F. Craievich, *Scr. Mater.*, **55**, 553–556 (2006).

18) A. Kuwabara, J. Katamura, Y. Ikuhara and T. Sakuma, *J. Am. Ceram. Soc.*, **85**, 2557–2561 (2002).

19) M. Yashima and S. Tsunekawa, *Acta Crystallogr., Sect. B: Struct. Sci.*, **61**, 161–164 (2006).

20) L. L. Chen, T. Mashimo, E. Omurzak, H. Okudera, C. Iwamoto and A. Yoshiasa, *J. Phys. Chem. C*, **115**, 9370–9375 (2011).

21) H. Ozturk and M. Durandurdu, *Phys. Rev. B*, **79**, 134111 (2009).

22) F. Maglia, M. Dapiaggi, I. Tredici, B. Maroni and U. Anselmi-Tamburini, *J. Am. Ceram. Soc.*, **93**, 2092–2097 (2010).

23) G. G. Stoney, *Proc. R. Soc. Lond.*, **82**, 172–175 (1909).

24) X. Feng, Y. Huang and A. J. Rosakis, *ASME J. Appl. Mech.*, **74**, 1276–1281 (2007).

25) R. E. Hann, P. R. Suitch and J. L. Pentecost, *J. Am. Ceram. Soc.*, **68**, C-285–C-286 (1985).

26) W. M. Kriven, W. L. Fraser and S. W. Kennedy, "The Martensitic Crystallography of Tetragonal Zirconia, Advances in Ceramics", Vol. 3, American Ceramic Society, Columbus, Ohio (1981) p. 82.